Novel Limit Cycles In Coupled Metronome Systems For Large Angles Through Non Linearity In The Van der Pol Equation

Birla Institute of Technology and Science, Pilani

Yashee Sinha

26th April 2021

Abstract

A set of metronomes can be coupled by keeping them on a base which is free to move, such as a swing. A single metronome system is a very popular example of a Van der Pol Oscillator which possesses a unique limit cycle in its phase space. However, for large angles, a fixed point can be found at 2π. For certain initial conditions, an n-coupled metronome system exhibits a smaller limit cycle in its phase space. In this study, we try to analyse the smaller limit cycle in terms of the analysis of fixed points in the free metronome system. We also provide a quantitative approximation to the frequency of the system when the non-linearity is introduced in the Van der Pol equation.

Acknowledgements

I thank my advisor Dr. Gaurav Dar for helping and guiding me throughout the process of working on this project. I thank the engineers at MATLAB for the software used for numerical simulations in this project. Finally, I thank my family for supporting me throughout this venture.

Contents

Chapter 1

Introduction

Van der Pol equations appear in many non linear systems. The equation is popularly described in the form:

$$\dot{x} = y \tag{1.1a}$$
$$\dot{y} = -x + \mu(1 - x^2)y \tag{1.1b}$$

One such system is a set of metronomes coupled by an oscillating base. For small angles, these systems show many notable features like synchronisation, unique limit cycles, phase locking, etc. Our study focuses on large amplitude oscillations of the metronome systems. Unlike the standard Van der Pol equation, the restoring force shows sinusoidal behaviour for large amplitudes. On an unrestricted domain of angles, the phase portraits of the systems show novel limit cycles and a discrete behaviour. Although such an unrestricted domain no longer models the physical metronome systems, the emergent behaviour can later on be generalised for a different physical system. Our aim, however, is not to discuss the physicality of the calculations and only deals with this novel mathematical behaviour.

1.1 Equations of motion

Our system includes a set of N metronomes placed on a moving base like a swing. Alone, these metronomes are the standard Van der Pol oscillators for small angles. A free metronome can be modeled as [1]:

$$\ddot{\phi} + \frac{mr_{c.m.}g}{I}\sin\phi + \mu_m\left[\left(\frac{\phi}{\phi_0}\right)^2 - 1\right]\dot{\phi} = 0 \tag{1.2}$$

where ϕ is the angle the pendulum makes with the vertical, I is the moment of inertia of the pendulum, m is the mass of the pendulum, $r_{c.m.}$ is the distance of the pendulum's center of mass from the pivot point, g is the acceleration of gravity. This will be an important point in our analysis for small coupling characteristics.

Our simulations are modelled on the N-metronomes on two coupled swings system as described in Martens et. al, 2013 [2]:

> We place N identical metronomes [with] a nominal beating frequency f on two swings, which can move freely in a plane. Oscillators within one population are coupled strongly by the motion of the swing onto

which the metronomes are attached. As f is increased, more momentum is transferred to the swing, effectively leading to a stronger coupling among the metronomes. A single swing follows a phase transition from a disordered state to a synchronized state as the coupling within the population increases

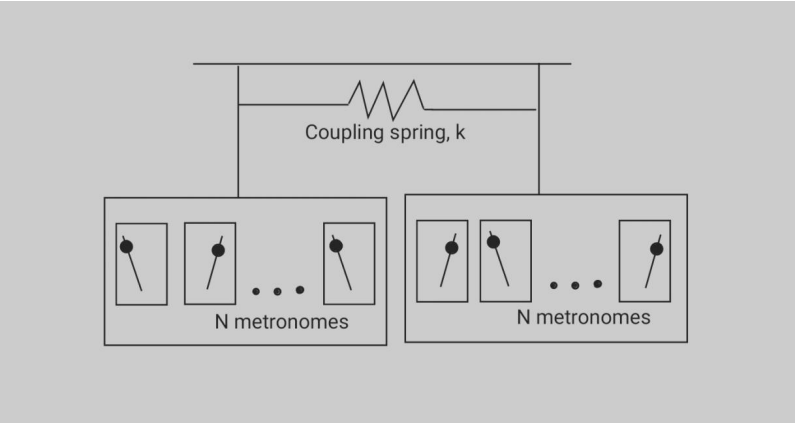

Figure 1.1: Martens' experiment setup

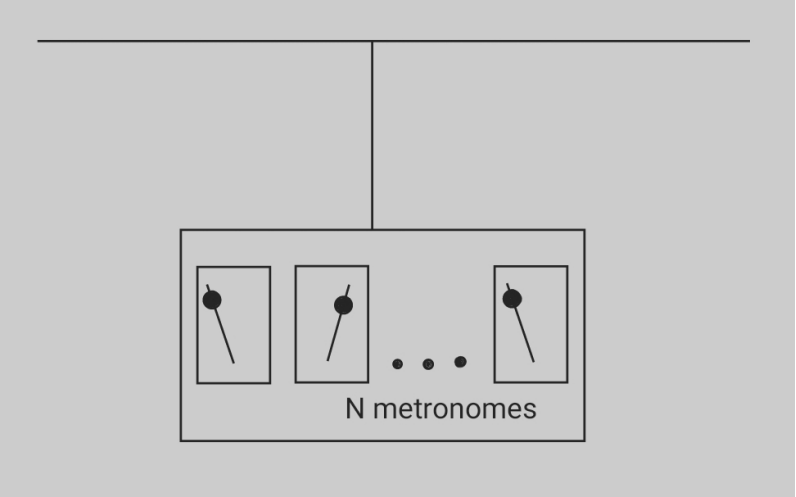

Figure 1.2: Our experiment setup

In Martens' experiment, two swings with N metronomes each are coupled with each other through a coupling spring (Figure 1.1). Our study, however, analyses a modified system with only a single swing carrying N-metronomes. (Figure 1.2). We will focus more on the effects of such synchronisation for large amplitudes. But we can easily borrow the equations of motion from Martens, substituting the coupling constant between two swings to be zero.

From [2, see Supplementary Information text], then, we have the following equations modelling our system:

$$\partial_\tau^2 \tilde{\Phi} = -\frac{\Omega^2}{\omega^2}\tilde{\Phi} - \mu_s\, \partial_\tau \tilde{\Phi} - \sum_{j=1}^{N} \partial_\tau^2 \sin\phi_j \tag{1.3a}$$

$$\partial_\tau^2 \phi_i = -\sin\phi_i - \mu_m \left(\left(\frac{\phi_i}{\theta_0} \right)^2 - 1 \right) \partial_\tau \phi_i - (\beta \cos\phi_i)\, \partial_\tau^2 \tilde{\Phi} \tag{1.3b}$$

where the list of symbols can be found in Appendix A.

ϕ_i is the angle made by the i-th metronome from its equilibrium position.

$\tilde{\Phi}$ is the angle made by the swing from its equilibrium, scaled appropriately to bring the equations of motion in a more familiar form, for our convenience. We will refer to it as just Φ from hereon, but it must be noted that this is not the true angle of the swing.

τ is the scaled time, where $\tau = \omega_0 t$, and ω is the natural frequency of a free metronome.

θ_0 is the metronome parameter that controls the damping, i.e., the damping term increases angular velocity for $\phi < \theta_0$ and decreases it for $\phi > \theta_0$.

Chapter 2

Numerical Simulations and Novel Behaviour

We have used MATLAB to simulate the Equation (1.3). The plots were made using MATLAB's inbuilt plotter. We will present the results found from the simulations in this chapter. The latter chapters will deal with analysing the systems to explain the results methodically, using a variety of methods like Poincaré–Lindstedt method, and Fourier-least squares method (FLSM). We aim to explain the novel behaviours and grant a qualitative solution to the problem.

Van der Pol Oscillators are usually known to exhibit a unique stable limit cycle in their phase space. For small μ_m and small angles, the Equation (1.2) has a globally stable limit cycle with an amplitude approximately equal to $2\theta_0$ [see 4, for example]. We will refer to this limit cycle as the standard Van der Pol limit cycle from hereon.

Now, we consider the system of N-metronomes coupled through a swing, as in Figure 1.2. We find that for small angles, the N-metronomes settle into the standard Van der Pol limit cycle. The swing also exhibits a unique stable limit cycle in its phase space. Figure 2.1 shows the limit cycles for various values of N. The θ_0 value is taken to be 1 radian, however the limit cycles will be exactly similar for typical value of 0.33 radians, albeit scaled down appropriately.

However, for large angles we find that some initial conditions give a smaller stable limit cycle centered at 2π (To show the limit cycle more clearly, the angles are wrapped around $[-\pi, \pi]$. However, Figure 2.3b shows the true limit cycle, as an example, centered around 2π.)

Figure 2.2 shows the stable limit cycles for $\theta_0 = 0.33$ and $N = 2$. However the amplitude of the smaller limit cycle is of the order of $1e-3$, which is too small to analyse meaningfully, and isn't even visible on the plot. But it can be seen that the swing has two limit cycles for large enough angles. We consider the case of $\theta_0 = 1$ in Figure 2.3. We find that as N increases, the number of limit cycles also increases.

Note: Every phase space in this paper should be assumed to represent N=2 if not otherwise mentioned. And it should be assumed that all swings start from rest.

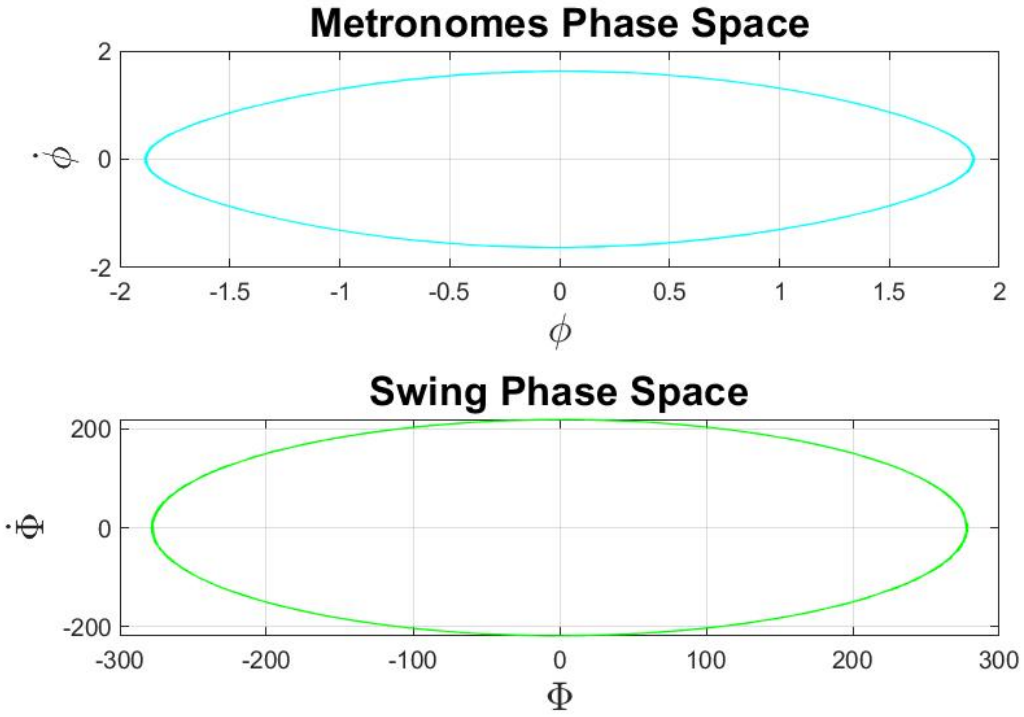
Metronomes Phase Space
$\dot{\phi}$
ϕ
Swing Phase Space
$\dot{\Phi}$
Φ

(a) N=2

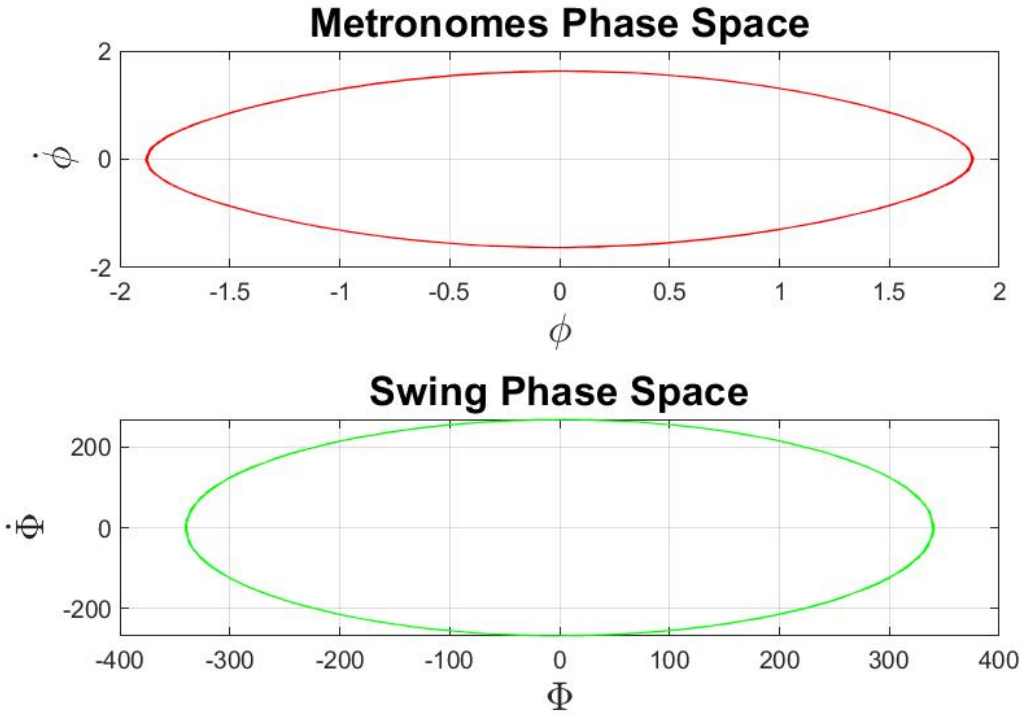
Metronomes Phase Space
$\dot{\phi}$
ϕ
Swing Phase Space
$\dot{\Phi}$
Φ

(b) N=3

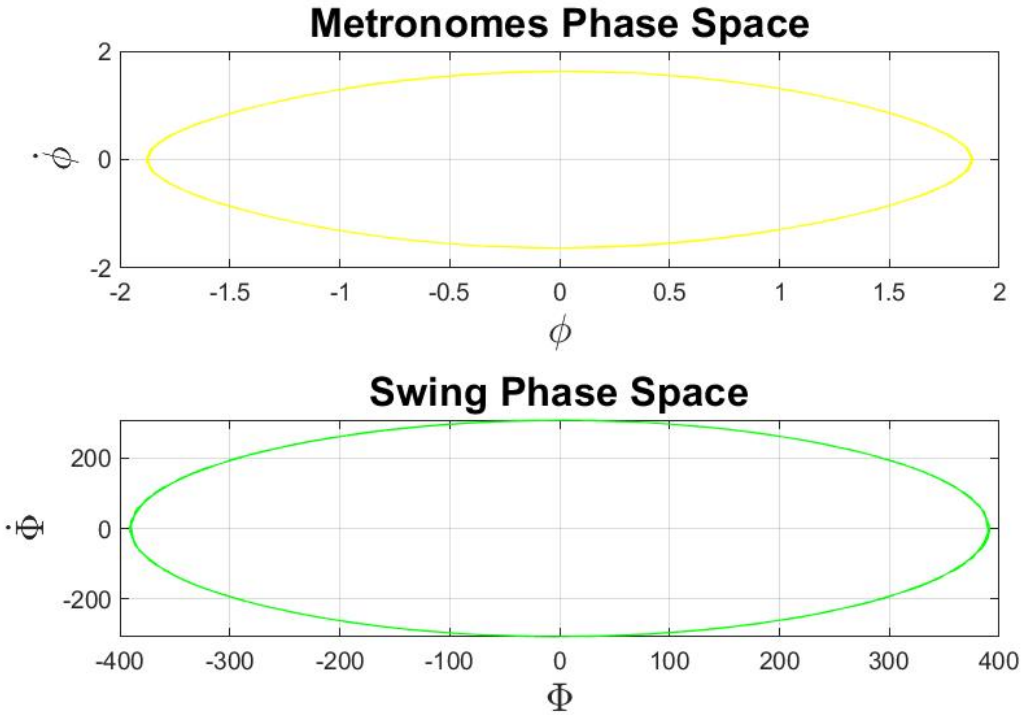

(c) N=4

Figure 2.1: Limit cycles for $\theta_0 = 1$, and initial conditions chosen in the region: $-1 < \phi < 1;\ -1 < \dot{\phi} < 1$

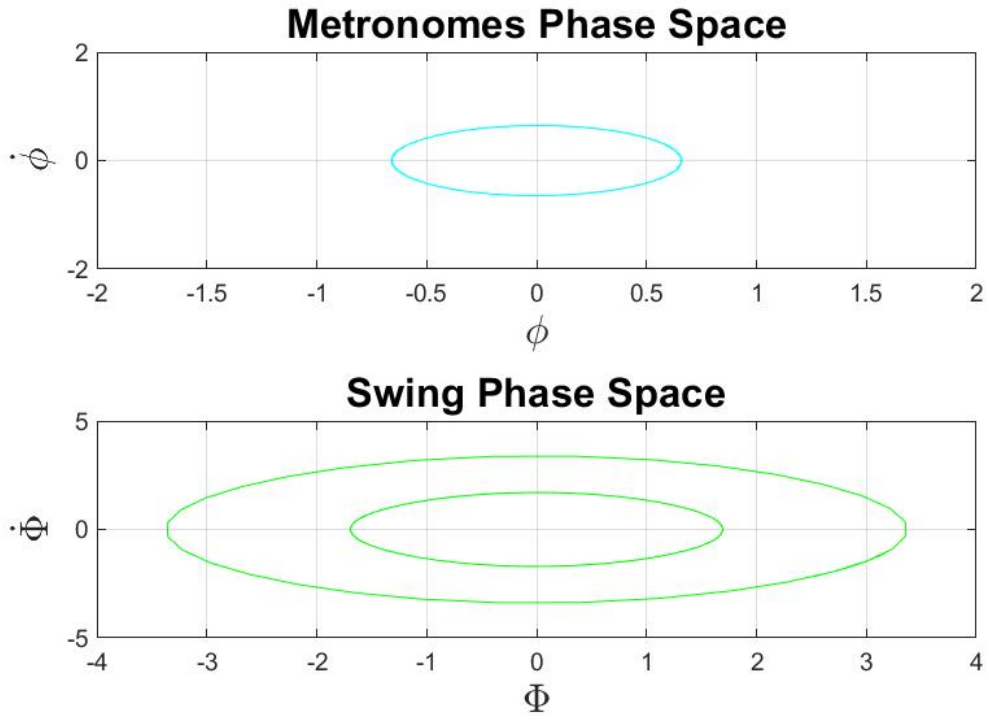

Figure 2.2: The limit cycles are generated for initial conditions in the region $(-2 \leq \phi \leq 2);\ (-2 \leq \dot{\phi} \leq 2)$

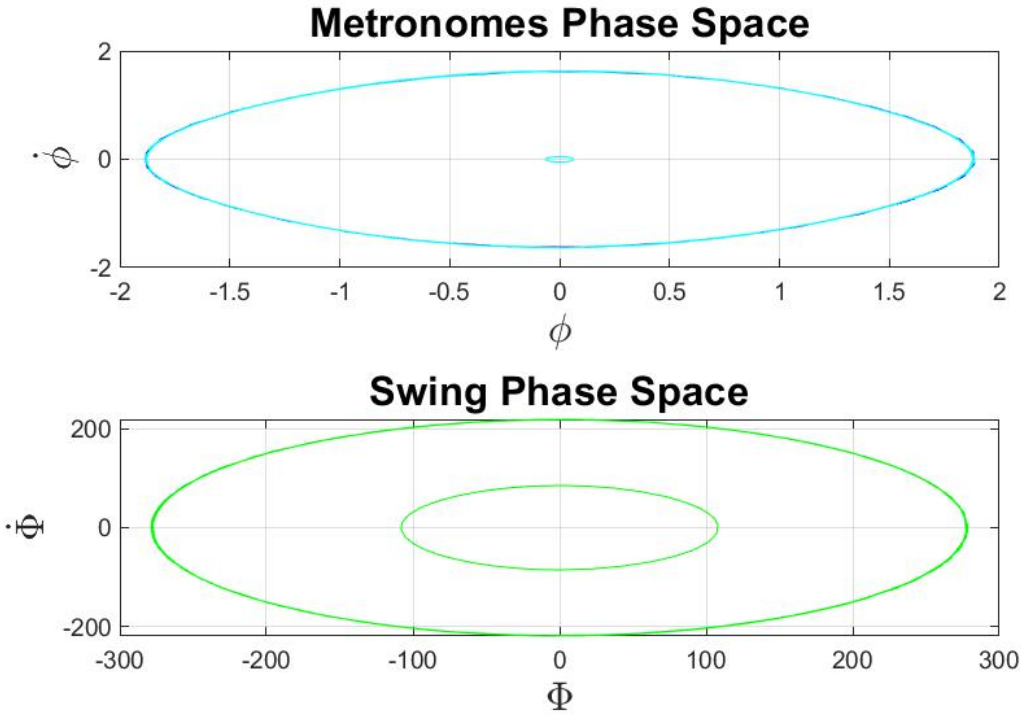
Metronomes Phase Space
$\dot{\phi}$
ϕ
Swing Phase Space
$\dot{\Phi}$
Φ

(a) N=2

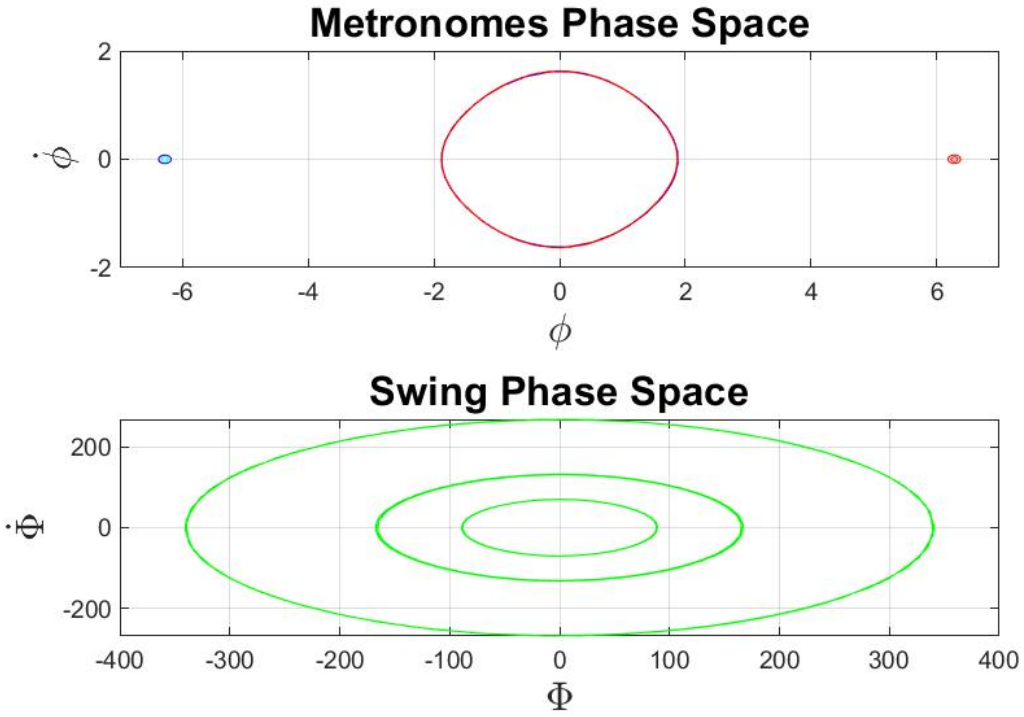
Metronomes Phase Space
$\dot{\phi}$
ϕ
Swing Phase Space
$\dot{\Phi}$
Φ

(b) N=3

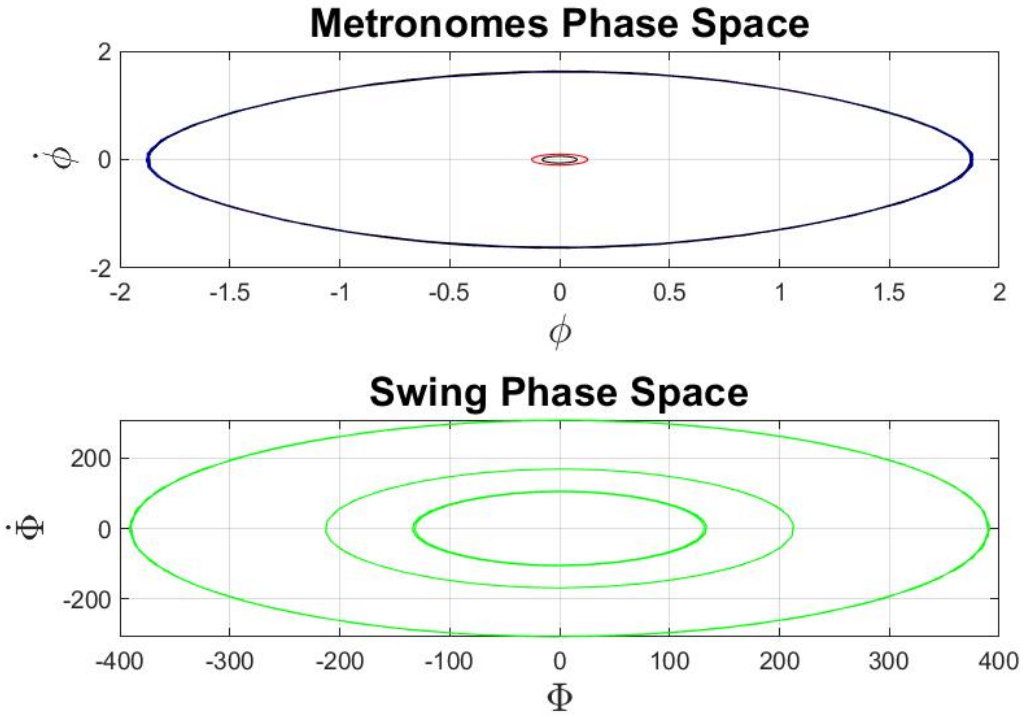

(c) N=4

Figure 2.3: Limit cycles for $\theta_0 = 1$, and initial conditions chosen in the region: $-2 < \phi < 2;\ -2 < \dot{\phi} < 2$

Chapter 3

Qualitative Analysis

3.1 Behavioural Dynamics for Metronomes

The best way to deal with this system is to find uncoupled equations which control the behaviour of the system. One clever to find such a behavioural equation is to exploit the extremely weak coupling in the system. According to the experimental parameters used by Martens, which can be found in the Appendix A, $\beta = 0.0005$. So in Equation (1.3b), we can safely ignore the coupled swing term for large angles.

The behavioural equations, then, turn out to be:

$$\ddot{\phi} + \sin\phi + \mu_m \left[\left(\frac{\phi}{\theta_0} \right)^2 - 1 \right] \dot{\phi} = 0 \tag{3.1}$$

which is very similar to Equation (1.2), the free Van der Pol equation.

We will deal with the equivalent system of equations:

$$\frac{d\phi}{d\tau} = \dot{\phi} \tag{3.2a}$$

$$\frac{d\dot{\phi}}{d\tau} = -\sin(\phi) - \mu_m \left[\left(\frac{\phi}{\theta_0} \right)^2 - 1 \right] \dot{\phi} \tag{3.2b}$$

3.1.1 Fixed Points

To deal with the system, we first look for limit cycles and fixed points of the system. We already know the existence of the standard Van der Pol Limit cycle around $[0, 0]$, but a quick look at Equation (3.2) suggests that due to the sinusoidal term, further fixed points exist at $[n\pi, 0]\ \forall\, n \in \mathbb{Z}$. For our convenience, we will focus our discussion only on π and 2π, however all odd and even multiples of π will follow the same results correspondingly.

To find the stability of the fixed point around 2π, we calculate the linearised form of Equation (3.2):

$$\frac{d}{d\tau} \begin{bmatrix} \phi \\ \dot{\phi} \end{bmatrix} = \begin{bmatrix} 0 & 1 \\ -\cos\phi - 2\,\dfrac{\mu_m\,\phi\,\dot{\phi}}{\theta_0^2} & -\mu_m \left[\left(\dfrac{\phi}{\theta_0} \right)^2 - 1 \right] \end{bmatrix} \begin{bmatrix} \phi \\ \dot{\phi} \end{bmatrix} \tag{3.3}$$

or

$$\frac{d}{d\tau}\boldsymbol{\phi} = \mathbf{J}\boldsymbol{\phi} \tag{3.4}$$

Assuming $\theta_0 = 1$, at $\boldsymbol{\phi} = [2\pi, 0]$, the Jacobian matrix, $\mathbf{J}$, and the eigenvalues of the corresponding $\mathbf{J}$ are listed below:

$$\mathbf{J} = \begin{bmatrix} 0 & 1 \\ -1 & -0.011(4\pi^2 - 1) \end{bmatrix}$$

$$\lambda_{\pm} = \frac{-33861 \pm i\sqrt{244534323679}}{160000} \tag{3.5}$$

The significant result to be noted here is that the real part of both the eigenvalues is negative around $\phi = 2\pi$. Hence, $[2\pi, 0]$ is a stable fixed point, where the trajectories spiral in towards it. Although we chose $\theta_0 = 1$, in reality this result holds for any $\theta_0 < 2\pi$. And since, θ_0 is the escapement term that is equal to half of the amplitude of a free metronome, $\theta_0 > \pi$ is a meaningless region, and can be safely ignored. A similar analysis around π will prove that the point $[\pi, 0]$ is an unstable fixed point.

Note: It's important to realise here that we are not restricting the domain of the angles. The equations of motion that we derived are valid in the region $-\pi < \phi < \pi$. Outside of this region, however, the dynamics may very well stop describing a metronome system. This is because the equations are not symmetrical in the transformation $\phi \to \phi + 2\pi$. However, our analysis ignores this discrepancy.

3.1.2 Basins of Attraction

Since Equation (3.1) is a two dimensional equation, we can meaningfully talk about the basins of attraction for the two fixed points in the phase space. Figure 3.1 shows that for large enough initial conditions, the system gets attracted towards the fixed point on either side of the limit cycle, shown in red. The blue points represent the initial conditions which get attracted towards the standard Van der Pol limit cycle. To be more accurate, however, the actual equation used to calculate the basins of attraction was:

$$\ddot{\phi} + \sin\phi + \mu_m \left[\left(\frac{\phi}{\theta_0} \right)^2 - 1 \right] \dot{\phi} = \beta A \tag{3.6}$$

where A is equal to the amplitude of the swing. This does not change the shape of the basins, but it does make the boundaries a better approximate for what we found in straightforward simulations of Equation (1.3). We will clarify why adding this term was justified in Section 3.2, and see how to quantify the amplitude of the swing in Section 4.2.

One way of looking at the system is to imagine elliptical trajectories around $[0, 0]$ similar to the standard Van der Pol. If any such trajectories intersect the $\phi = \pi$ line, the points transfer into the stable manifold of the fixed point, and not the limit cycle.

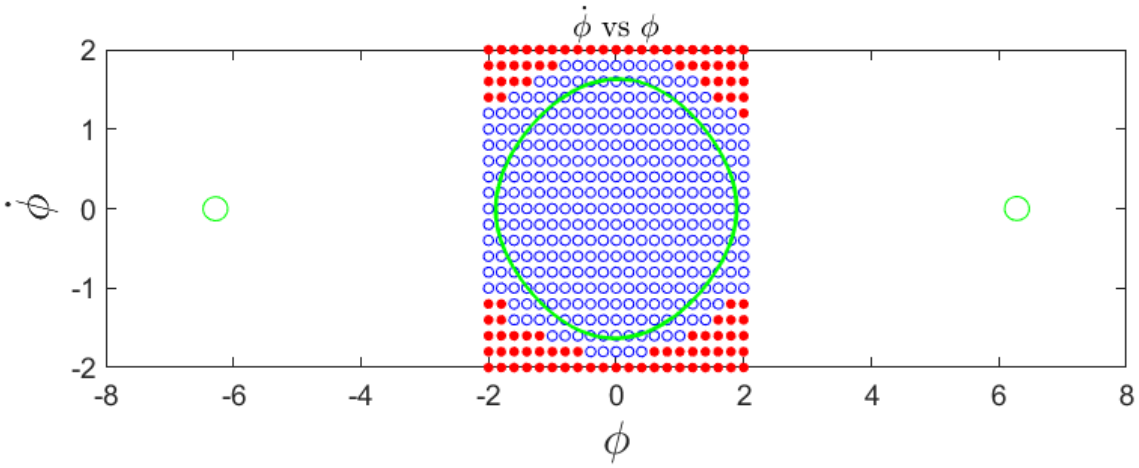

Red: Basin of attraction for the stable fixed points at -2π and 2π
Figure 3.1: *Blue*: Basin of attraction for the standard VdP-like limit cycle
Green: Limit cycles
The corresponding basins of attraction obtained from Equation (3.6). Please note that this is still only an approximation to the Equation (1.3b) which is in fact a two-dimensional equation.

3.2 Large and Small Amplitude Limit Cycles for Coupled Systems (LAL and SAL)

It's straightforward to carry on the analysis in the previous section for coupled systems. For any metronome whose initial conditions lie in the basin of attraction corresponding to the standard Van der Pol limit cycle, the metronomes stay in a limit cycle with large amplitude (hereon referred to as the Large Amplitude Limit Cycle or LAL). For any such metronomes, the amplitude of the LAL is large enough for the assumption made in Section 3.1 to be valid. The behavioural dynamics for such a metronome is described by Equation (3.1).

However, one can imagine a boundary at the $\phi = \pi$ line in Figure 3.1 that separates the two stable manifolds of this system (viz. the stable Large Amplitude Limit Cycle and the fixed point at $[2\pi, 0]$). And any metronome that crosses the boundary during its trajectory, such as those whose initial conditions lie in the red region of Figure 3.1, heads towards the stable fixed point. In such a case, the assumption that the angles of the metronomes are relatively large enough to ignore the coupled swing term no longer remains valid (refer Section 3.1). Hence as the trajectory spirals in towards $\phi = 2\pi$, the Equation (1.3b) take over and produce the Small Amplitude Limit Cycle (hereon referred to as SAL). One way to look at Equation (1.3b) is to recognize the swing term as the driving term, and analyse the equation as the forced Van der Pol equation. For such an analysis, we would require to understand the Swing's analytical solution which we shall do in Section 4.2.

But even before that, a quick way to confirm this idea of swing driving SAL is to note how the amplitude of such a forced Van der Pol equation would behave. By exploiting the idea that the free metronome equation, i.e. Equation (3.1), would spiral into the stable fixed point at $[2\pi, 0]$, the amplitude for any oscillation very close to the fixed point should be approximately equal to the amplitude of the non-zero oscillatory term in the RHS of Equation (1.3b). So, in fact, the amplitude of

N	Swing Amplitude (SA)	$\beta\times$ SA	Actual Amplitude of SAL
2	108.0439	0.054	0.064
3	94.1363	0.047	0.055
	167.168	0.0835	0.0995
4	91.658	0.0458	0.0535
	133.615	0.0668	0.0797
	212.636	0.1063	0.1265

Table 3.1: Approximations for amplitude of the SAL; $\beta = 0.0005$

the SAL should be approximately equal to ($\beta \times$ Amplitude of Swing), as you can see in Table 3.1. We also expect this approximation to get worse as the amplitude of the SAL increases, since the then the Van der Pol terms become more significant.

3.3 Behavioural Dynamics for Swing

Equation (1.3a) defines the governing behaviour for the swing. For N=2, the equation takes the form of:

$$\partial_\tau^2\tilde{\Phi} + \frac{\Omega^2}{\omega^2}\tilde{\Phi} + \mu_s\,\partial_\tau\tilde{\Phi} = -\partial_\tau^2(\sin\phi_1 + \sin\phi_2) \tag{3.7}$$

It is easy to recognise this equation as a forced damped equation. Once again, we can imagine the RHS term playing the role of the forcing term. Usually this forcing occurs due to the metronomes moving on the LAL. In fact, if one were to assume an analytical solution for the standard Van der Pol equation as $2\cos(\omega\tau)$[4], and run a Fourier analysis on Equation (3.7), a decent approximation for the swing's motion can be found. These ideas are elaborated more in Section 4.2.

In the next chapter, we will first attempt to approximate the frequency of the LAL. And move on from that to analyse the motion of the swing. However, the parameters used in this study happened to be very close to the natural frequency of Equation (3.7), i.e., $\frac{\Omega^2}{\omega^2}$. This introduces a much higher sensitivity to the amplitude as a function of frequency which our approximations might not fulfill. So while our approximations will be accurate for a two metronome system, with one metronome on the LAL and one on the SAL, the approximations fail miserably to predict the size of the limit cycle when more than one metronome is moving on the LAL.

3.4 LAL-Swing-SAL Model

To qualitatively deal with such systems, many times it's much better to view the system as distinct components driving each other to uncouple the equations. One model that we will apply in this paper is the LAL-Swing-SAL model. Basically, the metronomes in LAL can be seen as driving the swing through Equation (1.3a). Similarly, the swing can be seen as driving the metronomes moving on the SAL through Equation (1.3b).

So, these driving terms can always be replaced with an equivalent approximate analytical solution. This can be very useful in further analysing the systems and explaining quantitative results

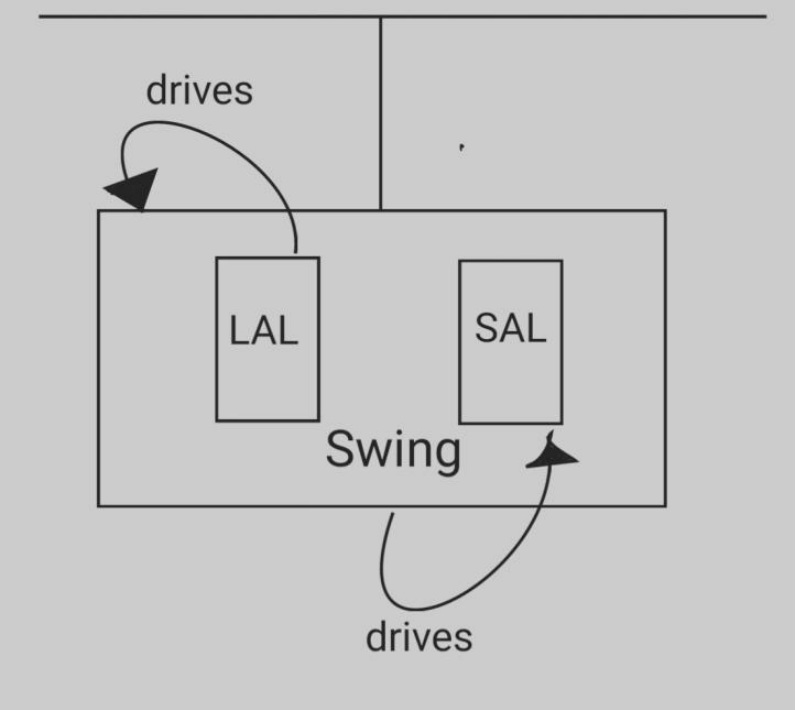

Figure 3.2: LAL-Swing-SAL model

Chapter 4

Quantitative Dynamics

4.1 Large Amplitude Limit Cycle (LAL)

A standard Van der Pol equation like Equation (1.1) has a popular analytical solution of the form of $x = 2\cos t$ [4]. However, due to the non-linear sinusoidal term in Equation (3.1) the frequency of the analytical solution is lesser. We shall assume that the amplitude of the solutions of Equation (3.1) remains the same. However, it can be kept in mind that the actual amplitude in a coupled system, due to the small coupling effect, is slightly lesser than 2. In our simulations, we found that the amplitudes of LAL in the coupled systems were of the order of 1.88.

4.1.1 Frequency Approximation of metronomes on the LAL

We will start by assuming a perturbation series for the metronome on the LAL.

$$\phi = \phi_0 + \mu_m \phi_1 + \mu_m^2 \phi_2 + \dots \tag{4.1}$$

First, we expand sin into its Mclaurin series. Equation (3.1), thus, becomes:

$$\begin{aligned}
&\left(\ddot{\phi_0} + \mu_m \ddot{\phi_1} + \mu_m^2 \ddot{\phi_2} + \dots\right) \\
&+\left((\phi_0 + \mu_m \phi_1 + \dots) - \frac{(\phi_0 + \mu_m \phi_1 + \dots)^3}{3!} + \frac{(\phi_0 + \mu_m \phi_1 + \dots)^5}{5!} + \dots\right) \\
&+\mu_m \left((\phi_0 + \mu_m \phi_1 + \mu_m^2 \phi_2 + \dots)^2 - 1\right)\left(\dot{\phi_0} + \mu_m \dot{\phi_1} + \mu_m^2 \dot{\phi_2} + \dots\right) = 0
\end{aligned}$$

On gathering the μ_m terms, we get the following system of equations:

$$\begin{aligned}
\ddot{\phi_0} + \phi_0 - \frac{\phi_0^3}{3!} + \frac{\phi_0^5}{5!} + \dots &= 0 \\
\mu_m\left(\dot{\phi_0}\left(\phi_0^2 - 1\right) + \frac{\phi_0^4 \phi_1}{24} - \frac{\phi_0^2 \phi_1}{2} + \dots\right) &= 0 \\
&\dots
\end{aligned}$$

or

$$\ddot{\phi_0} + \sin\phi_0 = 0 \tag{4.2a}$$

$$\mu_m \left(\dot{\phi_0} \left(\phi_0^2 - 1 \right) + \frac{\phi_0^4 \, \phi_1}{24} - \frac{\phi_0^2 \, \phi_1}{2} + \ldots \right) = 0 \tag{4.2b}$$

To find a decent approximation of the frequency of ϕ, we find the frequency of ϕ_0 in Equation (4.2a). The reason we can equate them is because for small μ_m, ϕ_0 gives the most significant contribution in Equation (4.1). To approximate the frequency of ϕ_0, we'll use a the Fourier-least squares method (FLSM) [3].

We start by assuming:

$$\phi_0 = \sum_{k=0}^{p} \left[\, a_{pk} \cos(k \, \omega_p \tau) + b_{pk} \sin(k \, \omega_p \tau) \, \right]$$

Now, we define:

$$\mathfrak{R} = \frac{d^2}{d\tau^2} \phi_0 + \sin(\phi_0)$$

$$\mathfrak{J} = \int_0^{\frac{2\pi}{\omega_p}} \mathfrak{R}^2 \, d\tau$$

Normally we would require to find a_k and b_k that minimised $\mathfrak{J}$ for different values of p. But to our convenience, we already suspect the solution would be similar to the form of $\phi_0 = 2\cos(\omega_1 \tau)$ because this is the analytical form of a standard Van der Pol oscillator. Putting this in $\mathfrak{J}$, and using numerical methods to integrate the expression[1], we get:

$$\mathfrak{J} = \int_0^{\frac{2\pi}{\omega_1}} \left(-2\omega_1^2 \cos\left(\omega_1 \tau\right) + \sin\left[2\cos\left(\omega_1 \tau\right) \right] \right)^2 d\tau$$

$$\mathfrak{J} = \int_0^{2\pi} \left(-2\omega_1^2 \cos\left(u\right) + \sin\left[2\cos\left(u\right) \right] \right)^2 \frac{du}{\omega_1} \qquad ; u = \omega_1 \tau$$

$$\mathfrak{J} = \int_0^{2\pi} \left(4\omega_1^4 \cos^2\left(u\right) + \sin^2\left[2\cos\left(u\right) \right] - 4\omega_1^2 \cos\left(u\right) \sin\left[2\cos\left(u\right) \right] \right) \frac{du}{\omega_1}$$

$$\mathfrak{J} = \frac{1}{\omega_1} \left(4\pi \, \omega_1^4 + 4.38927557863 - 14.494675352 \, \omega_1^2 \right)$$

The minimum of $\mathfrak{J}$ occurs at $\omega_1 = 0.764$.

From the simulations, we find that the actual frequency of a single metronome moving in the LAL is 0.779. So our calculated frequency is a decent approximate to

[1] WolframAlpha Language was used to perform these integrations and to find the minimum of the resulting expression.

our system. Further, we can also take into account the fact that in the simulations of the exact system, the amplitude of the LAL was in fact equal to 1.88 and not 2 due to various coupling factors that we had ignored. Then exactly the same method as above can be utilized while substituting $\phi_0 = 1.88\cos(\omega_1\tau)$ instead. The frequency achieved through this is $\omega_1 = 0.79$ which is a closer approximation to the actual frequency, as expected.

However, do note that our approximations are only valid for a single metronome moving on the LAL for $N = 2$ as we have assumed that the metronome is completely unaffected by the other metronome which is moving on the SAL. If both of the metronomes are travelling on the LAL or there are more than 2 metronomes, a more careful approach is required.

4.2 Swing

If we assume only one metronome is moving on the LAL, we find the behavioural equation for the swing takes the form:

$$\partial_\tau^2\Phi + \omega_r^2\Phi + \mu_s\,\partial_\tau\Phi = -\partial_\tau^2(\sin\phi) \tag{4.3}$$

where $\omega_r^2 = \dfrac{\Omega^2}{\omega^2}$.

We can decompose the RHS in a Fourier series with respect to $\omega\tau$, by assuming $\phi = 2\cos(\omega\tau)$. The Fourier Coefficients Calculator from *mathtools.com* was used for this purpose. After keeping only the significant terms of the Fourier series, we get:

$$\sin(2\cos(\omega\tau)) = 1.15344922\cos(\omega\tau) - 0.257881419\cos(3\omega\tau) + \dots$$

The required second derivative of this term can be written in the following form:

$$\begin{aligned} -\frac{d^2}{d\tau^2}\left[\sin(2\cos(\omega\tau))\right] &= -\frac{d^2}{d\tau^2}\left[a_1\cos(\omega\tau) + a_3\cos(3\omega\tau)\right] \\ \implies -\frac{d^2}{d\tau^2}\left[\sin(2\cos(\omega\tau))\right] &= \frac{a_1\omega^2}{2}\left(e^{i\omega\tau} + e^{-i\omega\tau}\right) + \frac{9\,a_3\omega^2}{2}\left(e^{3i\omega\tau} + e^{-3i\omega\tau}\right) \end{aligned}$$

where

$$\begin{aligned} a_1 &= 1.15344922 \\ a_3 &= -0.257881419 \end{aligned}$$

Now, we assume a Fourier series for Φ:

$$\Phi = \sum_{n=-\infty}^{\infty} y_n\, e^{ni\omega\tau}$$

We are assuming that the Fourier series is with respect to $\omega\tau$ and not τ because we expect the swing's limit cycle to have the same frequency as the metronomes for a stable system to exist.

Putting this in Equation (4.3), we get:

$$
\begin{aligned}
y_1 &= \frac{a_1\omega^2}{2}\,\frac{(\omega_r^2-\omega^2)-i\mu_s\omega}{(\omega_r^2-\omega^2)^2+\mu_s^2\omega^2}\\
y_{-1} &= \frac{a_1\omega^2}{2}\,\frac{(\omega_r^2-\omega^2)+i\mu_s\omega}{(\omega_r^2-\omega^2)^2+\mu_s^2\omega^2}\\
y_3 &= \frac{9\,a_3\omega^2}{2}\,\frac{(\omega_r^2-9\omega^2)-3i\mu_s\omega}{(\omega_r^2-9\omega^2)^2+9\mu_s^2\omega^2}\\
y_{-3} &= \frac{9\,a_3\omega^2}{2}\,\frac{(\omega_r^2-9\omega^2)+3i\mu_s\omega}{(\omega_r^2-9\omega^2)^2+9\mu_s^2\omega^2}
\end{aligned}
$$

This implies:

$$
\begin{aligned}
\Phi = {} & a_1\omega^2\,\frac{(\omega_r^2-\omega^2)}{(\omega_r^2-\omega^2)^2+\mu_s^2\omega^2}\cos(\omega\tau) + a_1\omega^2\,\frac{\mu_s\omega}{(\omega_r^2-\omega^2)^2+\mu_s^2\omega^2}\sin(\omega\tau)\\
& + 9\,a_3\omega^2\,\frac{(\omega_r^2-9\omega^2)}{(\omega_r^2-9\omega^2)^2+9\mu_s^2\omega^2}\cos(3\omega\tau) + 9\,a_3\omega^2\,\frac{3\mu_s\omega}{(\omega_r^2-9\omega^2)^2+9\mu_s^2\omega^2}\sin(3\omega\tau)
\end{aligned}
\tag{4.4a}
$$

$$
\Phi = 102.284\cos(\omega\tau) + 0.2897\cos(3\omega\tau) + 1.8635\sin(\omega\tau) - 0.00002\sin(3\omega\tau)
\tag{4.4b}
$$

The first term of the series is the dominating term, since its coefficient happens to be very large. For $\omega = 0.779$, i.e. a single metronome travelling on the LAL in an $N = 2$ system, and the other values the same as described in Appendix A, the first term, viz. the amplitude of Φ, from Equation (4.4b) is equal to -102.28.

From our numerical simulations, we found the actual amplitude the swing was approximately equal to -108.09, which is a very good approximation! Of course, this system is very close to resonance, so we can't use our calculated frequency from Section 4.2.

The minus sign implies that the swing is out of phase with the metronome on the LAL, which is what we observe in the simulations too. (see Figure 4.1, which plots the two phases with each other, where phase is defined as $\frac{\dot{\phi}}{\phi}$ for the metronome and $\frac{\dot{\Phi}}{\Phi}$ for the swing)

Note: this analytical solution for the motion of the swing also does not hold for any case other than an N=2 system with one of the metronomes moving on the LAL, since it is dependent on the accuracy of the frequency of the LAL (or system). However, using more rigorous methods, a better solution can be found for more cases.

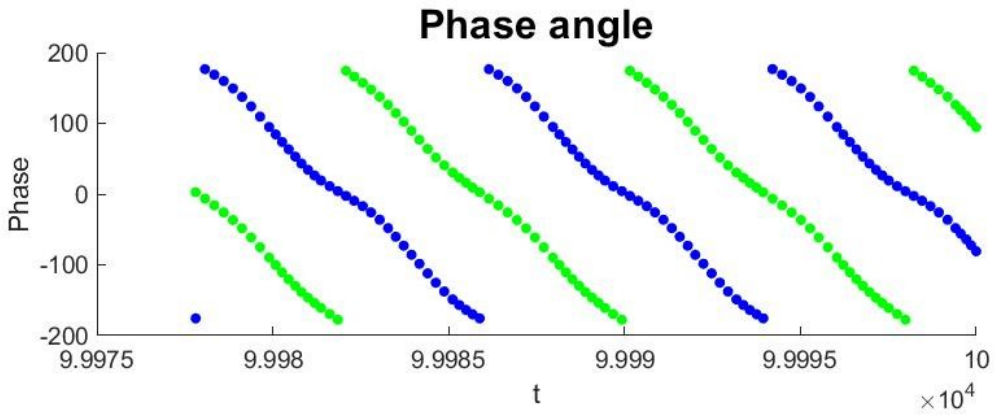

Figure 4.1: *Blue*: The phase v/s time of the metronome moving on the LAL
Green: The phase v/s time of the swing
The phase difference between the two phases is approximately equal to π.

Chapter 5

Limit Cycles in N Metronomes

To generalise what we have seen, and predict the number of limit cycles that exist in each phase space as N increases, we utilise the LAL-Swing-SAL model from Section 3.4.

We can imagine that each metronome can individually head towards a smaller or larger limit cycle. Since according to our model each metronome moving in the LAL is driving the swing, the size of the limit cycle of the swing increases discretely with increase in the the number of metronomes in the LAL. And since we have already seen in Table 3.1 that the size of the Small Amplitude Limit cycles are proportional to the size of the swing, we can note a discrete increase of the size of the SAL with the increase in the number of metronomes.

Table 5.1 compares the amplitude of the swing and number of metronomes in the LAL for various N.

N	Number of metronomes in LAL	Amplitude of the Swing
2	1	108.78
	2	278.67
3	1	106
	2	167.17
	3	340.7745
4	1	100.54
	2	133.61
	3	210.204
	4	391.24

Table 5.1: The Amplitude of the limit cycle of the swing, and hence the SAL, is directly proportional to the discrete number of metronomes moving in the LAL, hence showing discrete limit cycles

5.1 Possibility of Oscillation Death

In the entire paper, we have intentionally left out the case where both the metronomes should head towards the smaller limit cycles. Our simulations suggest that the limit cycles of such a system, if they are indeed limit cycles, are of the order of 10^{-7}. Such

limit cycles are so small, they might as well be at rest. Hence, the possibility exists that oscillation death occurs for the initial conditions that produce SALs.

5.2 Unexplained Degeneracy of Certain Orbits

Another property of these limit cycles that was found in the simulations but not discussed in this paper was the existence of degenerate orbits. We sampled 50 random initial conditions on the system, while increasing the value of N. It was found that for higher values of N some limit cycles in the phase space of the metronome were extremely close to each other. Two examples for $N = 4$ and $N = 5$ are shown in Section 5.2. In our analysis, no significant reason was provided for such a phenomenon, and we have considered them mostly degenerate in our discussions till now. As expected, changing the amplitude of the limit cycle even slightly alters the frequency of the system by a small amount and since the system is close to its natural resonance, the swing shows an amplified change in the limit cycles in its phase space. However, this might hint to the possibility of a more nuanced approach to the system.

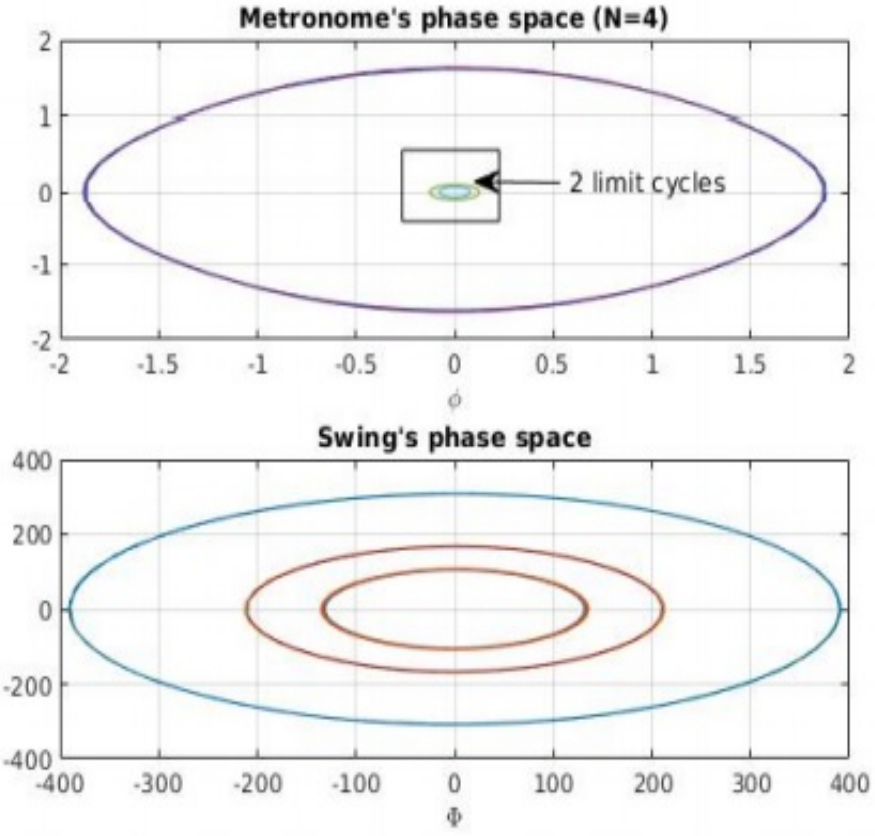

(a) N=4

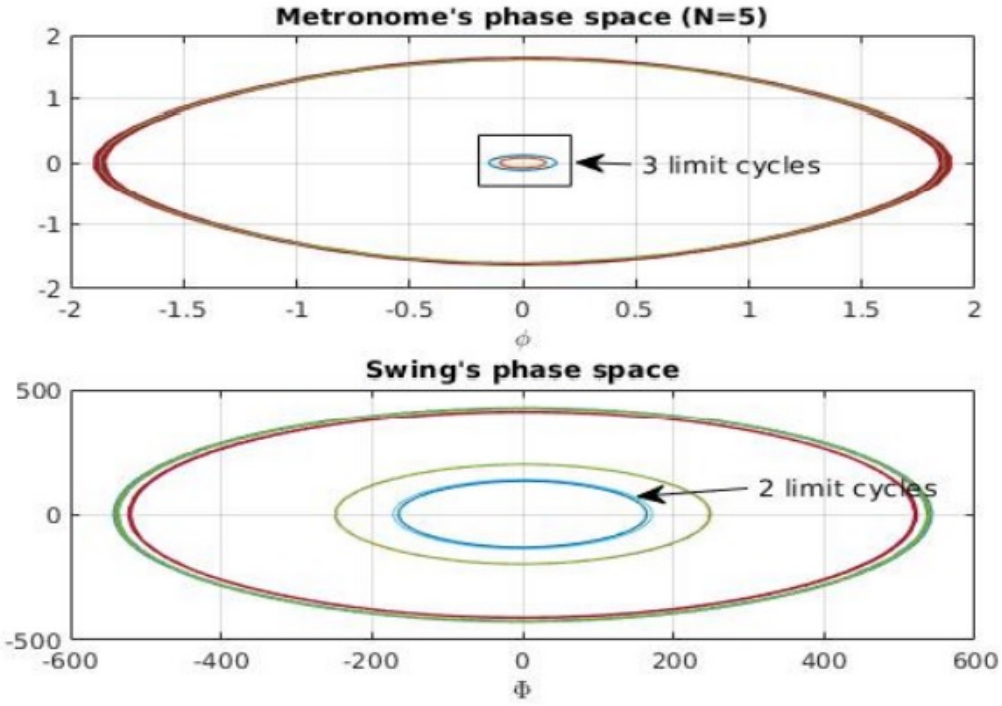

(b) N=5

Figure 5.1: Limit cycles for $\theta_0 = 1$, and 50 random initial conditions chosen in the region: $-2 < \phi < 2;\ -2 < \dot{\phi} < 2$

Chapter 6

Conclusions

In this study, we found that if we do not restrict the domains of the equations of motion of coupled metronomes, smaller limit cycles can be observed to form around $\phi = 2\pi$. Also, due to the non linearity of the sinusoidal restoring term in the Van der Pol equation, the frequency of the system is no longer $\tau = \omega_0 t$, but is reduced. An approximation for the amplitudes of the various components and the frequency of the system was found, too.

However, the quantitative analysis to find approximate analytical solutions presented in this study were limited to $N = 2$. For a better analysis one can apply more rigorous numerical methods to better approximate the system for higher Ns.

Also, this study ignores the fact that the domain of the angles for the equations of motion should be restricted to $-\pi < \phi < \pi$ to model the physical system of metronomes. Further research can look into other systems that such an unrestricted domain might model. Specifically, one may attempt to design a circuit which follows these equations on all domains. The applications of such a system, if it exists, could be studied. One such application could be novel ways for Injection lockings to take place. A further study into the phenomena of oscillation deaths and degenerate orbits can be fruitful in such a case.

Appendix A

List of Symbols

From [2]:

ϕ_i	Angular position of i-th metronome with respect to the equilibrium position
$\tilde{\Phi}$ or Φ	Angular position of the swing with respect to the equilibrium. It is scaled by $\frac{x_0}{L}$ such that $\tilde{\Phi} = \frac{x_0}{L}\Phi$
ω_0^2	$\frac{mgr_{cm}}{I} = 8.61 rad/s$
μ_m	$\frac{\nu_m}{I\omega_0} = 0.011$
μ_s	$\frac{\nu_s}{M\omega_0} = 0.00016$
Ω^2	$\frac{g}{L}$
x_0	$\frac{mr_{cm}}{M}$
r_{cm}	Distance of the Center of mass of the metronome from its pivot
ω_r^2	$\frac{\Omega^2}{\omega^2} = 0.6$

Appendix B

Calculations for the swing

From Section 4.2, when we put

$$\Phi = \sum_{n=-\infty}^{\infty} y_n \, e^{ni\omega\tau}$$

in the equation,

$$\partial_\tau^2 \Phi + \omega_r^2 \Phi + \mu_s \, \partial_\tau \Phi = \frac{a_1 \omega^2}{2} \left(e^{i\omega\tau} + e^{-i\omega\tau} \right) + \frac{9 \, a_3 \omega^2}{2} \left(e^{3i\omega\tau} + e^{-3i\omega\tau} \right)$$

We get the following expression:

$$\sum_{n=-\infty}^{\infty} \left(-n^2\omega^2 + \omega_r^2 + i\mu_s n\omega \right) y_n \, e^{ni\omega\tau} = \frac{a_1 \omega^2}{2} \left(e^{i\omega\tau} + e^{-i\omega\tau} \right) + \frac{9 \, a_3 \omega^2}{2} \left(e^{3i\omega\tau} + e^{-3i\omega\tau} \right)$$

By comparing both sides, and keeping only the non zero coefficients we find,

$$\begin{aligned}
\left(-n^2\omega^2 + \omega_r^2 + i\mu_s n\omega \right) y_1 \, e^{i\omega\tau} &= \frac{a_1 \omega^2}{2} \, e^{i\omega\tau} \\
\left(-n^2\omega^2 + \omega_r^2 + i\mu_s n\omega \right) y_{-1} \, e^{-i\omega\tau} &= \frac{a_1 \omega^2}{2} e^{-i\omega\tau} \\
\left(-n^2\omega^2 + \omega_r^2 + i\mu_s n\omega \right) y_3 \, e^{3i\omega\tau} &= \frac{9 \, a_3 \omega^2}{2} e^{3i\omega\tau} \\
\left(-n^2\omega^2 + \omega_r^2 + i\mu_s n\omega \right) y_{-3} \, e^{-3i\omega\tau} &= \frac{9 \, a_3 \omega^2}{2} e^{-3i\omega\tau}
\end{aligned}$$

From this, one can derive the following values:

$$\begin{aligned}
y_1 &= \frac{a_1 \omega^2}{2} \, \frac{(\omega_r^2 - \omega^2) - i\mu_s\omega}{(\omega_r^2 - \omega^2)^2 + \mu_s^2 \omega^2} \\
y_{-1} &= \frac{a_1 \omega^2}{2} \, \frac{(\omega_r^2 - \omega^2) + i\mu_s\omega}{(\omega_r^2 - \omega^2)^2 + \mu_s^2 \omega^2} \\
y_3 &= \frac{9 \, a_3 \omega^2}{2} \, \frac{(\omega_r^2 - 9\omega^2) - 3i\mu_s\omega}{(\omega_r^2 - 9\omega^2)^2 + 9\mu_s^2 \omega^2} \\
y_{-3} &= \frac{9 \, a_3 \omega^2}{2} \, \frac{(\omega_r^2 - 9\omega^2) + 3i\mu_s\omega}{(\omega_r^2 - 9\omega^2)^2 + 9\mu_s^2 \omega^2} \\
y_n &= 0 \quad \forall n \notin \{1, -1, 3, -3\}
\end{aligned}$$

And, finally, the expression for Φ can be alternatively written as:

$$\sum_{n=-\infty}^{\infty} y_n\, e^{ni\omega\tau} = y_0 + \sum_{n=1}^{\infty} \left[(y_n + y_{-n}) \cos(n\omega\tau) + (y_n - y_{-n}) \sin(n\omega\tau) \right]$$

$$\begin{aligned} \implies \Phi = {} & a_1\omega^2 \, \frac{(\omega_r^2 - \omega^2)}{(\omega_r^2 - \omega^2)^2 + \mu_s^2\omega^2} \cos(\omega\tau) + a_1\omega^2 \, \frac{\mu_s\omega}{(\omega_r^2 - \omega^2)^2 + \mu_s^2\omega^2} \sin(\omega\tau) \\ & + \, 9\, a_3\omega^2 \, \frac{(\omega_r^2 - 9\omega^2)}{(\omega_r^2 - 9\omega^2)^2 + 9\mu_s^2\omega^2} \cos(3\omega\tau) + 9\, a_3\omega^2 \, \frac{3\mu_s\omega}{(\omega_r^2 - 9\omega^2)^2 + 9\mu_s^2\omega^2} \sin(3\omega\tau) \end{aligned}$$

Bibliography

[1] James Pantaleone. "Synchronisation Of Metronomes". In: *American Journal of Physics* 992.70 (2002). DOI: http://dx.doi.org/10.1119/1.1501118.

[2] Erik Andreas Martens et al. "Chimera states in mechanical oscillator networks". In: *Proceedings of the National Academy of Sciences* 110.26 (2013), pp. 10563–10567. ISSN: 0027-8424. DOI: 10.1073/pnas.1302880110. eprint: https://www.pnas.org/content/110/26/10563.full.pdf. URL: https://www.pnas.org/content/110/26/10563.

[3] Constantin Bota. "Approximate Periodic Solutions for Oscillatory Phenomena Modelled by Nonlinear Differential Equations". In: *Mathematical Problems in Engineering* 2014 (2014). DOI: https://doi.org/10.1155/2014/513473.

[4] Steven H. (Steven Henry) Strogatz. *Strogatz, Steven H. (Steven Henry) author. Nonlinear Dynamics and Chaos : with Applications to Physics, Biology, Chemistry, and Engineering.* Westview Press, a member of the Perseus Books Group, 2015.